Characterization of Filovirus Protein–Protein Interactions in Mammalian Cells Using Bimolecular Complementation

Yuliang Liu, Sasha Stone, and Ronald N. Harty

Department of Pathobiology, School of Veterinary Medicine, University of Pennsylvania, Philadelphia

The virion protein 40 (VP40) and nucleoprotein (NP) of Ebola (EBOV) and Marburg viruses (MARV) play key roles during virion assembly and egress. The ability to detect interactions between VP40-VP40, VP40-NP, and NP-NP and follow these complexes as they traffic through mammalian cells would enhance our understanding of the molecular events leading to filovirus assembly and budding, and provide new insights into filovirus replication and pathogenesis. Here, we successfully employed a bimolecular complementation (BiMC) approach to visualize interactions between EBOV and MARV VP40-VP40, NP-NP, and VP40-NP proteins and localize these protein complexes in mammalian cells using confocal microscopy. We demonstrate that VP40-VP40 complexes localized predominantly at the plasma membrane, whereas VP40-NP and NP-NP complexes displayed a more dispersed pattern throughout the cytoplasm. As expected based on previous findings, efficient interactions between EBOV or MARV VP40-VP40 proteins were independent of L-domains PTAPPEY and PPPY, respectively. In contrast, the formation of EBOV or MARV VP40-VP40 complexes was dependent on the previously characterized LPLGVA and LPLGIM motifs of EBOV and MARV VP40 proteins, respectively, indicating that these motifs are important for VP40 oligomerization and subsequent budding. These results highlight the feasibility and usefulness of the BiMC approach as a strategy to further characterize both filovirus protein interactions as well as filovirus-host interactions in real time in the natural environment of the cell.

Ebola (EBOV) and Marburg viruses (MARV) belong to the *Filoviridae* family and are the causative agents of rapidly progressive, hemorrhagic fevers with high mortality rates among humans and nonhuman primates [1]. To date, there is no approved vaccine nor pharmacological therapy available to protect or treat individuals infected with filoviruses [1, 2]. Filoviruses are enveloped, nonsegmented, negative-strand RNA viruses with ~19-kilobase genomes containing 7 sequentially arranged genes. Genes encode 7 structural proteins: nucleoprotein (NP), virion proteins (VP35, VP40, VP30, and VP24), polymerase protein, transmembrane glycoprotein (GP), and for all EBOV species, a nonstructural, secreted glycoprotein (sGP) is also encoded [1, 3]. VP40 is necessary for the redistribution of the nucleocapsids from cytoplasmic inclusions to the sites of particle assembly and budding [3], as well as for recruitment of GP to the VP40-positive peripheral clusters where budding takes place [4].

Expression of VP40 alone in mammalian cells results in egress of filamentous virus-like particles (VLPs) that closely resemble authentic filovirus particles [5–8]. Late (L) domains within EBOV VP40 and within MARV VP40 (mVP40) and NP play an important role in the budding process of filoviruses by recruiting host factors to promote efficient egress [3, 9–11]. Indeed, the $_{7}$PTAPPEY$_{13}$ motif in EBOV VP40 (eVP40), the $_{16}$PPPY$_{19}$ motif in mVP40, and the recently identified $_{603}$PSAP$_{606}$ motif in MARV NP (mNP) are critical for

Potential conflicts of interest: none reported.

Presented in part: 5th International Symposium on Filoviruses, Tokyo, Japan, 18–21 April 2010. Abstract 7.

Correspondence: Ronald N. Harty, PhD, Department of Pathobiology, School of Veterinary Medicine, University of Pennsylvania, 3800 Spruce St, Philadelphia, PA 19104 (rharty@vet.upenn.edu).

The Journal of Infectious Diseases 2011;204:S817–S824

0022-1899 (print)/1537-6613 (online)/2011/204S3-0011$14.00
DOI: 10.1093/infdis/jir293

efficient production of filovirus particles [6, 12–16]. In addition to L-domains, oligomerization of VP40 was shown to be important for intracellular transport, membrane binding, and virus particle formation and egress [17, 18]. In addition to VP40, filovirus GP and NP proteins were shown to contribute to efficient egress of filovirus particles [4, 6, 7, 10, 14, 19–21]. For example, coexpression of EBOV NP (eNP) or GP with eVP40 significantly enhanced release of VLPs from mammalian cells [21, 22], and MARV NP (mNP) was shown recently to enhance budding of MARV by recruiting host Tsg101 via a C-terminal PSAP L-domain motif [10]. Thus, coordinated interactions among filovirus proteins are essential for efficient virion assembly and egress. A better understanding of the molecular interplay among filoviral proteins in mammalian cells is warranted and may facilitate the development of novel antiviral therapeutics.

To begin to address gaps in our understanding of intracellular interaction sites and trafficking patterns of filovirus protein complexes in the cell, we successfully employed a bimolecular complementation (BiMC) approach [23–25] to detect, visualize, and map wild-type (WT) and mutant filovirus protein-protein interactions in live mammalian cells. Indeed, this approach was used to visualize VP40-VP40, VP40-NP, and NP-NP interactions for both EBOV and MARV. The BiMC technique is based on an underlying principle that a reporter protein (eg, enhanced yellow fluorescent protein [EYFP] used in this study) can be split into 2 separate inactive components, which are then genetically fused to potentially interacting protein partners (eg, filovirus proteins). An interaction between these partners results in essentially irreversible reconstitution of an active EYFP, allowing for direct visualization and quantitation in living cells [23–25]. Advantages of the BiMC technique are that it enables characterization of protein-protein interactions in the natural cellular environment and allows for the detection and recording of weak or transient interactions [24, 25]. Our findings provide proof of principle of the feasibility of using the BiMC approach to map the intracellular locations and trafficking patterns of filovirus protein complexes in live cells.

MATERIALS AND METHODS

Cells, Antibodies, and Plasmids

293T (human embryonic kidney) cells were maintained in Dulbecco's modified Eagle medium (DMEM; Invitrogen) supplemented with 10% fetal calf serum (FCS; Hyclone) and 1 × penicillin-streptomycin (Invitrogen) at 5% CO_2 at 37°C. Rabbit antiserum against eVP40 was described previously [26]. Mouse monoclonal antibody against FLAG epitope (Sigma-Aldrich) was used according to the manufacturer's instructions. Plasmids eVP40-WT, eVP40-ΔLPLGVA, mVP40-WT (kindly provided by S. Becker, Marburg, Germany), mVP40-ΔLPLGIM and pCAGGS-eNP were previously described [21, 26]. Plasmid pCAGGS-mNP was kindly provided by S. Becker (Marburg, Germany), via C. Basler (Mt. Sinai Med. Ctr., New York) and E. Muehlberger (Boston Univ., Boston MA). Sequences of all EBOV viral proteins were derived from Zaire EBOV strain Zaire 1995 (GenBank accession No: AY354458.1), and those of all MARV viral proteins were derived from Lake Victoria MARV strain Musoke (GenBank accession No: NC_001608). Plasmid pCS2–containing full-length *Venus* EYFP was generously provided by R. Eisenberg and G. Cohen (University of Pennsylvania School of Dental Medicine). All recombinant plasmids containing WT or mutant VP40 or NP fused with the N- or C-termini of EYFP were constructed by standard polymerase chain reaction (PCR) and cloning techniques using the pCAGGS expression vector.

Transfection and Confocal Microscopy

Transfection and confocal microscopy were performed as previously described [26]. Human 293T cells were grown on glass coverslips in 6-well plates and were transfected with the indicated plasmids using Lipofectamine reagent (Invitrogen). At 4 hours posttransfection (pt), cell culture supernatant was replaced with fresh DMEM containing 10% FCS. At 24 hours pt, cells were washed twice with phosphate-buffered saline (PBS; pH 7.2) and fixed with cold methanol-acetone (1:1, v/v) for 10 minutes at room temperature. Cells were washed as described above and subsequently stained with 4′, 6′-diamidino-2-phenylindole (DAPI) for 10 minutes at room temperature. Cells were washed 4 times with PBS and affixed to glass slides with Prolong Antifade (Invitrogen/Molecular Probes). Slides were viewed by an LSM-510 Meta confocal microscope (Carl Zeiss).

VLP Budding Assay and Western Blotting

Transfection, VLP isolation, and Western blotting were performed as described previously [26]. Equal amounts of proteins in cell extracts and purified VLPs were subjected to sodium dodecyl sulfate polyacrylamide gel electrophoresis (SDS-PAGE) and then analyzed by Western blotting as described previously [26].

RESULTS AND DISCUSSION

Generation and Expression of EYFP-Fusion Proteins

The basic premise of the BiMC strategy is illustrated in Figure 1 [23–25]. A series of plasmids were constructed to express EBOV or MARV VP40 or NP proteins joined in-frame to either the N-terminal fragment of EYFP (YN or NYFP), or the C-terminal fragment of EYFP (YC or CYFP) (Figure 1). Expression of all EYFP-filovirus fusion proteins in transfected cells was confirmed by Western blotting using appropriate antisera (Figure 2). Fusion of the EYFP fragments to the N-termini of WT or mutant VP40 proteins did not appear to alter protein expression, nor the well-characterized, L-domain-dependent budding properties of

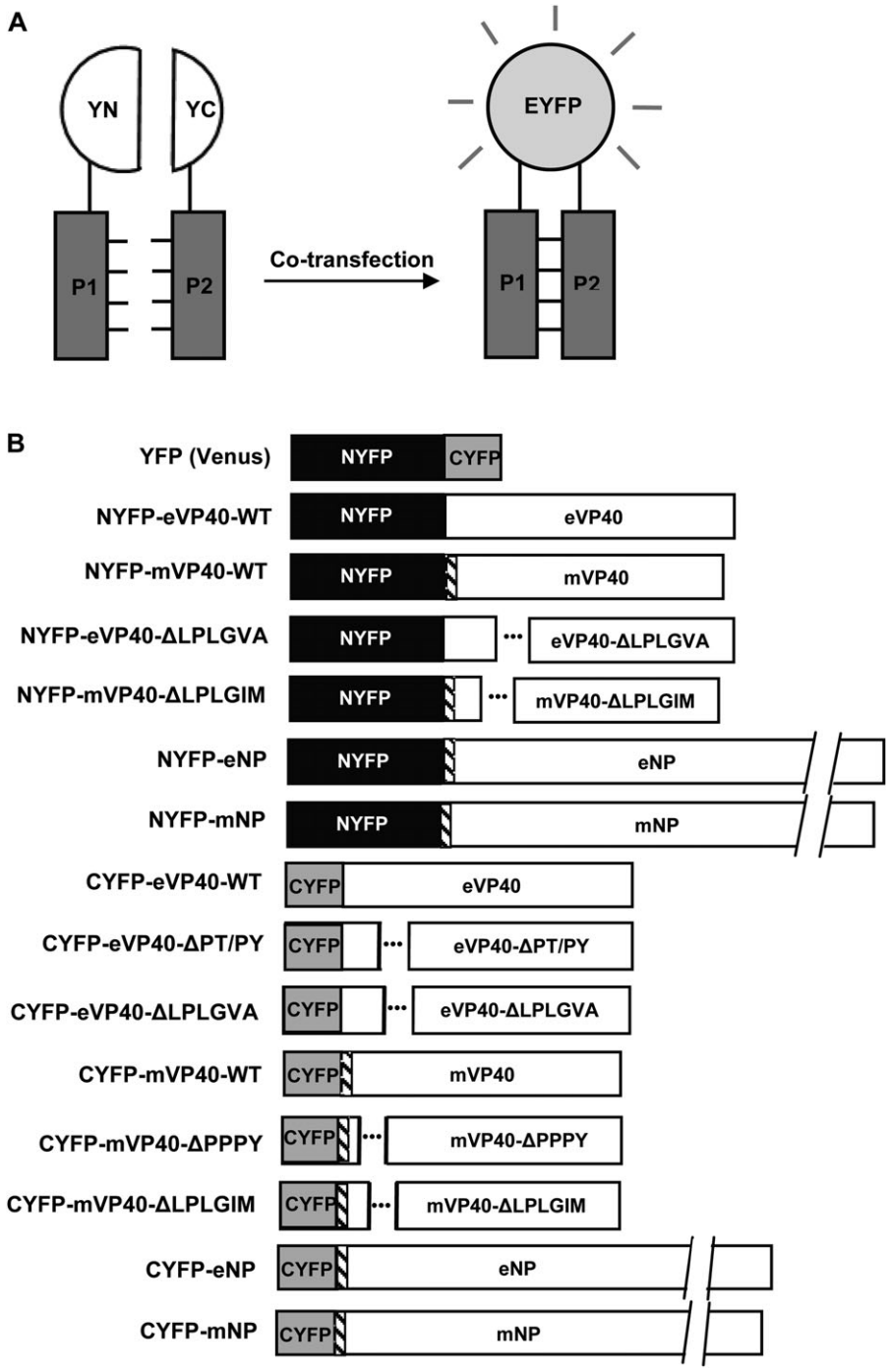

Figure 1. Diagram of Enhanced Yellow Fluorescent Protein fusion proteins. (*A*) Schematic diagram of the basic principle of the bimolecular complementation (BiMC) assay. Enhanced yellow fluorescent protein (EYFP) is split into 2 nonfluorescent fragments (denoted YN [aa 1–173] and YC [aa 174–239]), which are joined in-frame to 2 proteins of interest (designated P1 and P2). Interaction of P1 with P2 leads to reconstitution of EYFP and a resultant fluorescent signal when exposed to ultraviolet light. (*B*) Schematic diagram and names of the constructs used in this manuscript. The hatched box represents the location of a FLAG epitope tag, and the dotted line represents amino acid deletions as indicated.

these viral matrix proteins (Figure 2). As an example, CYFP-eVP40-WT and CYFP-eVP40-ΔPT/PY were both expressed in cell extracts (Figure 2); however, only CYFP-eVP40-WT was able to bud efficiently as a VLP (Figure 2), whereas budding of CYFP-eVP40-ΔPT/PY L-domain mutant was defective (Figure 2). Unmodified eVP40-WT (Figure 2) was included as a control. Similar findings were obtained using mVP40-WT (control), CYFP-mVP40-WT, and CYFP-mVP40-ΔPPPY (Figure 2).

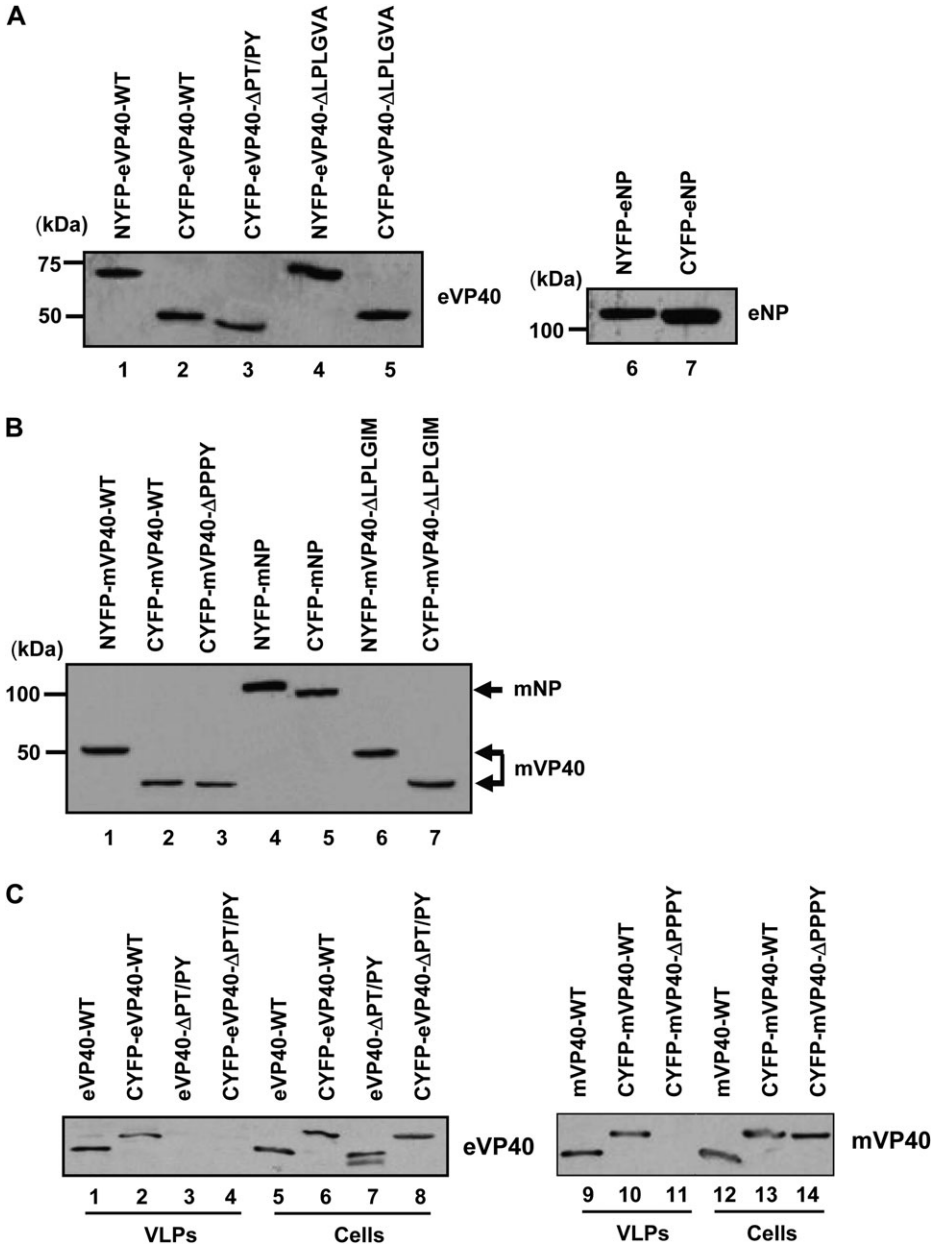

Figure 2. Expression and budding of EYFP fusion proteins. (*A*) Western blots to detect expression of all Ebola virus (EBOV) fusion proteins. (*B*) Western blots to detect expression of all Marburg virus (MARV) fusion proteins. (*C*) Budding assay and western blot of EBOV and MARV virion protein 40 (VP40), and CYFP-VP40 fusion proteins.

VP40-VP40 Interactions

First, we sought to detect a VP40-VP40 interaction using the BiMC assay. We used fusion proteins expressing WT and deletion mutants of both eVP40 and mVP40 (Figure 3). It should be noted that human 293T cells singly transfected with any of the EYFP fusion plasmids yielded no fluorescent signal (Liu and Harty, data not shown). Human 293T cells were cotransfected with NYFP-eVP40-WT + CYFP-eVP40-WT, and the cells were examined by confocal microscopy at 24 hours pt for EYFP fluorescence (Figure 3). A strong, reproducible EYFP signal was observed indicative of an eVP40-eVP40 interaction (Figure 3). As expected, the eVP40-eVP40 complexes were enriched at the cell surface and displayed a pattern of filamentous-like membrane projections (Figure 3). A similar pattern was observed in cells expressing NYFP-mVP40-WT + CYFP-mVP40-WT (Figure 3). Notably, in addition to the cell surface fluorescence, we consistently observed a strong fluorescent signal in a perinuclear pattern in cells expressing NYFP-mVP40-WT + CYFP-mVP40-WT, but not in cells expressing NYFP-eVP40-WT + CYFP-eVP40-WT (Liu and Harty, data not shown). Whether this reproducible difference in the fluorescent patterns of eVP40 and mVP40 complexes represents distinct

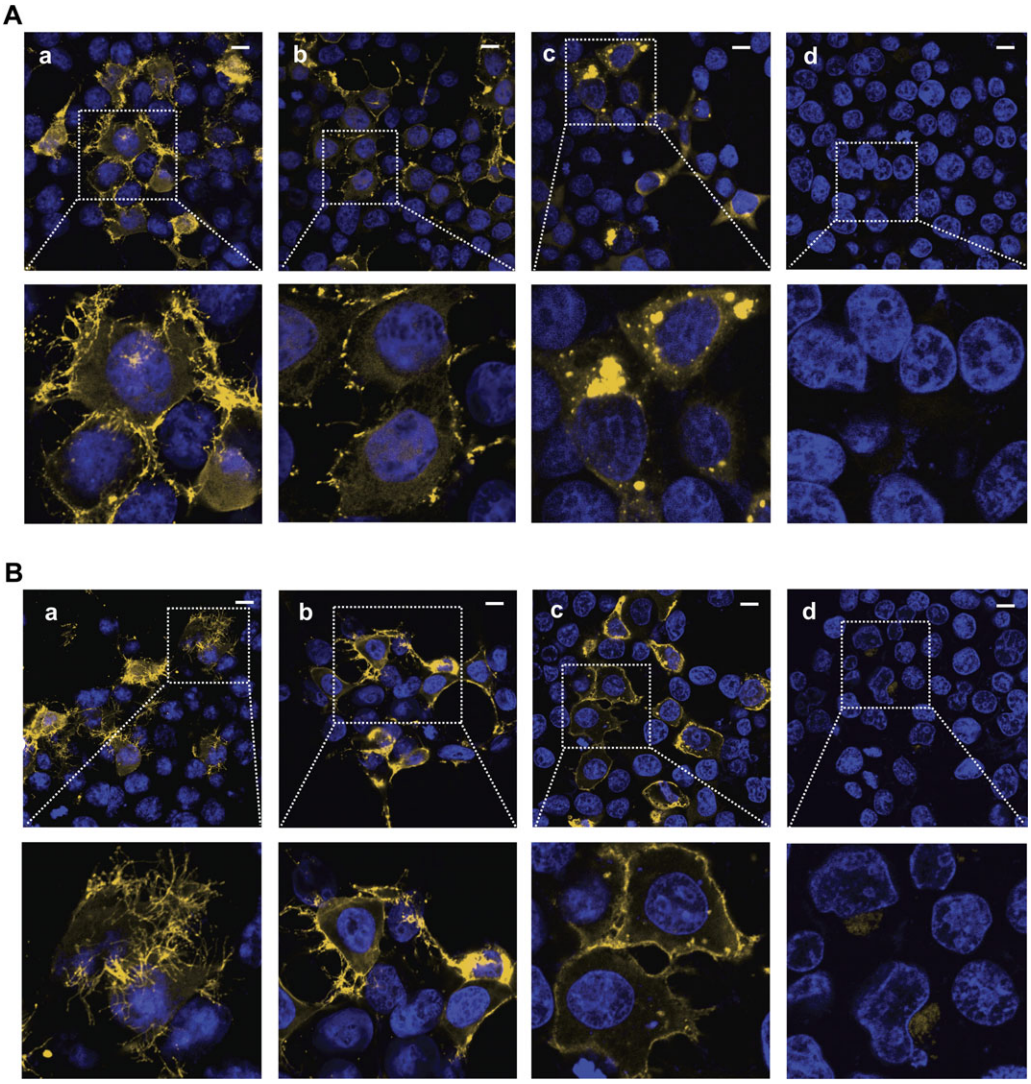

Figure 3. Bimolecular complementation assay to detect Ebola virus and Marburg virus virion protein 40 (VP40)-VP40 interactions. (*A*) Ebola virus (EBOV) VP40 proteins. Human 293T cells were cotransfected with: a) NYFP-eVP40-WT + CYFP-eVP40-WT, b) NYFP-eVP40-WT + CYFP-eVP40-ΔPT/PY, c) NYFP-eVP40-WT + CYFP-eVP40-ΔLPLGVA, or d) NYFP-eVP40-ΔLPLGVA + CYFP-eVP40-ΔLPLGVA and examined by confocal microscopy at 24h posttransfection. The dotted square represents the enlarged image shown below the original image. (*B*) Marburg virus (MARV) VP40 Proteins. Human 293T cells were cotransfected with: a) NYFP-mVP40-WT + CYFP-mVP40-WT, b) NYFP-mVP40-WT + CYFP-mVP40-ΔPPPY, c) NYFP-mVP40-WT + CYFP-mVP40-ΔLPLGIM, or d) NYFP-mVP40-ΔLPLGIM + CYFP-mVP40-ΔLPLGIM and examined by confocal microscopy at 24 h p.t.. The dotted square represents the enlarged image shown below the original image. The white bar represents 10 μm.

intracellular transport pathways for these complexes, or distinct homo-oligomerization properties of eVP40 and mVP40 remains to be determined.

Next, we assessed the ability of 2 different VP40 deletion mutants to interact with WT forms of both EBOV and MARV VP40. We reasoned that the L-domain deletion mutants of eVP40 (eVP40- ΔPT/PY) and mVP40 (mVP40-ΔPPPY) should still interact with their corresponding WT VP40 partner and display a fluorescent pattern similar to that observed for VP40-VP40 WT complexes, because the L-domains function in host protein recruitment. In contrast, use of the previously described ΔLPLGVA and ΔLPLGIM mutants of eVP40 and mVP40, respectively would likely alter the pattern of fluorescence observed for VP40-VP40 WT complexes, because these and adjacent sequences appear to be required for efficient oligomerization, membrane localization, and egress of VP40 [18, 26]. Indeed, NYFP-eVP40-WT + CYFP-eVP40-ΔPT/PY complexes (Figure 3) and NYFP-mVP40-WT + CYFP-mVP40-ΔPPPY complexes (Figure 3) were enriched at the cell surface yielding a fluorescent signal that was slightly reduced, but overall similar to that described for EBOV and MARV VP40-WT complexes. In contrast, cells expressing CYFP-eVP40-ΔLPLGVA + NYFP-eVP40-WT (Figure 3) revealed a highly punctate pattern of fluorescence that was dramatically different from that observed

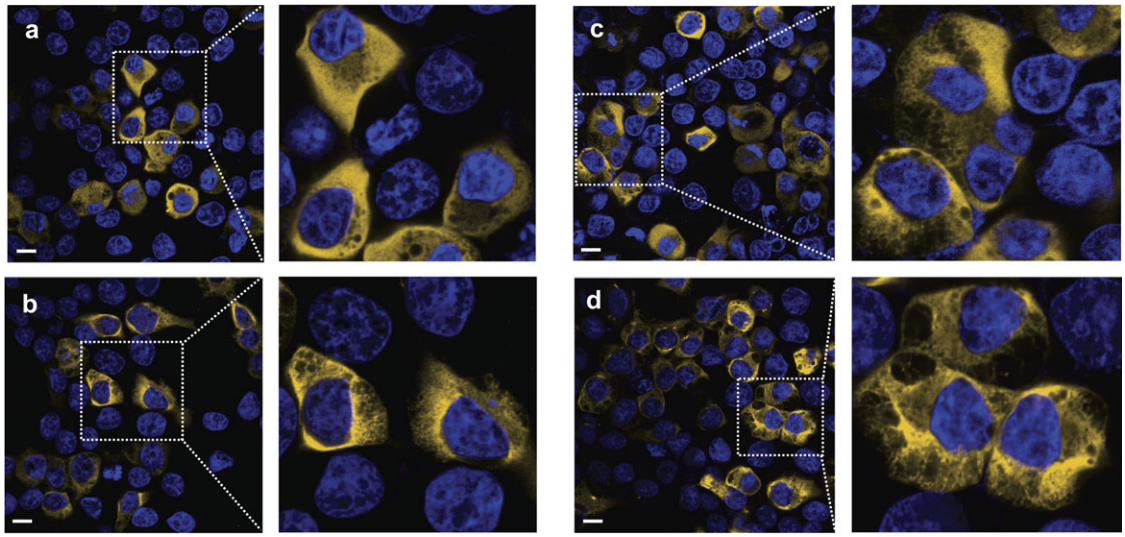

Figure 4. Bimolecular complementation assay to detect Ebola virus and Marburg virus nucleoprotein (NP)-NP and virion protein 40 (VP40)-NP interactions. Human 293T cells were cotransfected with: *a*) NYFP-eNP + CYFP-eNP, *b*) NYFP-eNP + CYFP-eVP40-WT, *c*) NYFP-mNP + CYFP-mNP, or *d*) NYFP-mVP40-WT + CYFP-mNP and examined by confocal microscopy at 24 h p.t. The dotted square represents the enlarged image shown to the right of the original image. The white bar represents 10 μm.

for eVP40-WT complexes (panel a). Interestingly, the mVP40-ΔLPLGIM mutant also retained the ability to interact with mVP40-WT (Figure 3); however, the pattern of fluorescence exhibited by these complexes was only slightly punctate, with more predominant staining at the plasma membrane (Figure 3). Notably absent however was the presence of abundant filamentous membrane projections clearly visible for mVP40-WT complexes (Figure 3). Lastly, virtually no fluorescent signal was observed in cells coexpressing either NYFP-eVP40-ΔLPLGVA + CYFP-eVP40-ΔLPLGVA (Figure 3), or NYFP-mVP40-ΔLPLGIM + CYFP-mVP40-ΔLPLGIM (Figure 3), indicating that these sequences are critical for eVP40 and mVP40 self-interactions.

In sum, these findings using the BiMC approach correlated well with our previous characterization of the eVP40-ΔLPLGVA and mVP40-ΔLPLGIM mutants [26], suggesting that these sequences are indeed critical for VP40 self-interactions and intracellular localization. In further support of these findings, Hoenen et al reported recently that mutating residues W95 or L96 (within the LPLGVA motif) of eVP40 resulted in impaired oligomerization of eVP40, defective intracellular transport to the plasma membrane, and decreased egress of eVP40 VLPs [18].

VP40-NP and NP-NP Interactions

Next, we sought to determine whether the BiMC approach could be used to detect VP40-NP and NP-NP interactions and visualize these protein complexes in mammalian cells. VP40-NP interactions have been shown to be important for both virus assembly and enhanced budding of VLPs and virus particles [8, 10, 21, 27], whereas NP-NP interactions are essential for RNP assembly in the cytoplasm of infected cells [27]. Human 293T cells were cotransfected with plasmids expressing NYFP-eNP + CYFP-eNP (Figure 4), NYFP-eNP + CYFP-eVP40-WT (panel b), NYFP-mNP + CYFP-mNP (panel c), or NYFP-mVP40-WT + CYFP-mNP (panel d), and fluorescent cells were observed at 24 hours posttransfection. We observed bright EYFP fluorescence in a predominantly diffuse, cytoplasmic pattern for both VP40-NP and NP-NP complexes (Figure 4), with a low level of staining for VP40-NP complexes at the plasma membrane (data not shown). The intracellular patterns observed for VP40-NP and NP-NP complexes for both EBOV and MARV (Figure 4) were clearly distinct from those observed for VP40-VP40 complexes (Figure 3). In addition, we observed that the eVP40-ΔLPLGVA and mVP40-ΔLPLGIM deletion mutants interacted with eNP and mNP, respectively, yielding a similar pattern of cytoplasmic fluorescence and suggesting that the LPLGVA and LPLGIM sequences are not essential for the formation of VP40-NP complexes (Liu and Harty, data not shown).

Notably, the diffuse cytoplasmic pattern of fluorescence observed for both NYFP-eNP + CYFP-eNP (Figure 4) and NYFP-mNP + CYFP-mNP (Figure 4), differed from the more speckled-type pattern observed when antibodies were used to detect NP [28]. Whether this difference reflects the location of the EYFP fragment at the N-terminus of eNP and mNP remains to be determined. It should be noted that the addition of increasing amounts of unmodified eNP or mNP to cells coexpressing NYFP-eNP + CYFP-eNP or NYFP-mNP + CYFP-mNP, respectively, did not significantly alter the diffuse

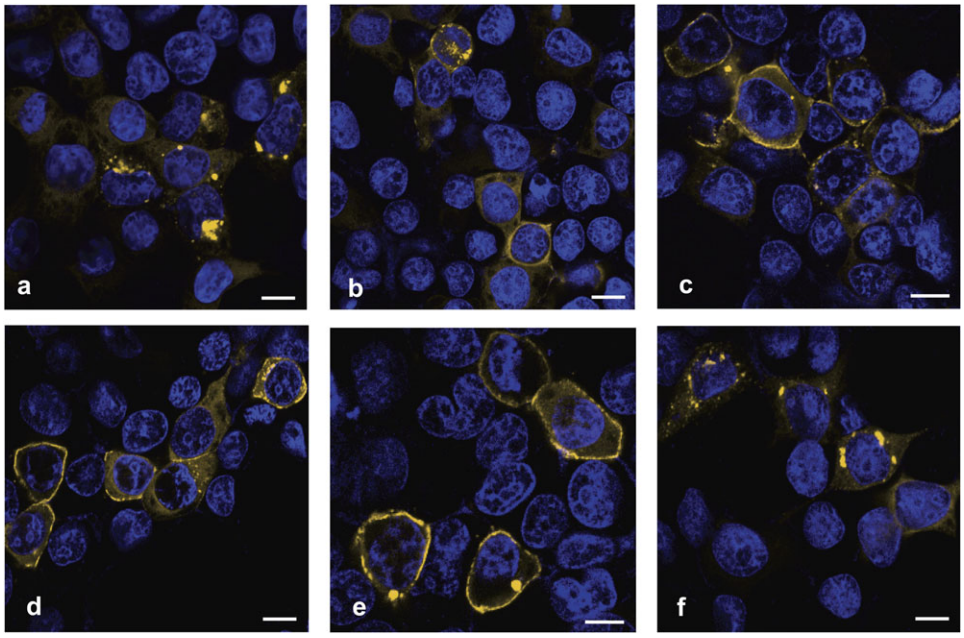

Figure 5. Relocalization of NYFP-eVP40-WT + CYFP-eVP40-ΔLPLGVA complexes by overexpression of eVP40-WT. Human 293T cells were cotransfected with equivalent amounts of NYFP-eVP40-WT + CYFP-eVP40-ΔLPLGVA in the presence of 0.0 μg (*a*), 0.3 μg (*b*), 0.6 μg (*c*), 1.2 μg (*d*), or 2.0 μg (*e*) of unmodified eVP40-WT. As a negative control, 2.0 μg of pCAGGS empty vector was added (f). Cells were examined by confocal microscopy at 24 h posttransfection. The white bar represents 10 μm.

cytoplasmic pattern of fluorescence observed in Figure 4 (Liu and Harty, data not shown).

Overexpression of eVP40-WT Relocalizes NYFP-eVP40-WT + CYFP-eVP40-ΔLPLGVA Complexes

We have shown previously that overexpression of eVP40-WT was able to rescue the budding defective phenotype of deletion mutant eVP40–ΔLPLGVA, resulting in the egress of VLPs containing both eVP40-WT and eVP40–ΔLPLGVA [26]. Thus, it was of interest to determine whether overexpression of unmodified eVP40-WT would alter the intracellular localization of NYFP-eVP40-WT + CYFP-eVP40–ΔLPLGVA complexes (Figure 3) to more closely resemble that observed for NYFP-eVP40-WT + CYFP-eVP40-WT complexes (Figure 3). Toward this end, human 293T cells were cotransfected with constant amounts of NYFP-eVP40-WT + CYFP-eVP40-ΔLPLGVA plasmids along with increasing amounts (0.0, 0.3, 0.6, 1.2, and 2.0 μg) of unmodified eVP40-WT plasmid (Figure 5). In a control dish, 2.0 μg of pCAGGS empty vector was added (Figure 5). Consistent with results described in Figure 3, the fluorescent pattern exhibited by NYFP-eVP40-WT + CYFP-eVP40-ΔLPLGVA complexes in the absence of excess eVP40-WT was primarily punctate in nature, with little to no plasma membrane staining (Figure 5). Interestingly, on cotransfection of increasing amounts of eVP40-WT plasmid, the intracellular localization of the NYFP-eVP40-WT + CYFP-eVP40-ΔLPLGVA complexes shifted to a more plasma membrane-enriched pattern (Figure 5). Indeed, the overall intensity and sharpness of the plasma membrane staining exhibited by the NYFP-eVP40-WT + CYFP-eVP40-ΔLPLGVA complexes increased in a dose-dependent manner. In stark contrast, cotransfection of 2.0 μg of pCAGGS empty vector did not alter the fluorescent pattern formed by NYFP-eVP40-WT + CYFP-eVP40-ΔLPLGVA complexes (Figure 5). Thus, these results suggest that expression of excess eVP40-WT mediated the mobilization of the existing eVP40-WT/eVP40-ΔLPLGVA complexes from the perinuclear aggregates to the plasma membrane, likely resulting in enhanced release and rescue of budding VLPs observed previously [26].

In sum, our results using the BiMC approach provide proof of principle that this strategy can be used to dissect further the interplay not only between filovirus protein-protein interactions, but also filovirus-host interactions (Liu and Harty, manuscript submitted) that are crucial for virus replication, budding, and pathogenesis. Importantly, detection and mapping of these protein-protein interactions and complexes will be assessed in real time in the natural biological environment of the cell. Future studies will undoubtedly lead to new insights into the mechanistic similarities and differences between EBOV and MARV replication, and may aid in the identification of novel targets for the development of antiviral therapeutics.

Funding

This work was supported in by National Institutes of Health (grants AI077014 and AI090284); and the University of Pennsylvania Research Foundation (funding to R. N. H.).

Acknowledgments

We thank Dr. Atsushi Okumura for helpful discussions. We thank Drs. S. Becker, C. Basler, and E. Muehlberger, G. Olinger, R. Eisenberg, G. Cohen, and D. Atanasiu for generously providing us with reagents. We also thank Andrea Stout and Jasmine Zhao for their expert assistance with confocal microscopy.

References

1. Ascenzi P, Bocedi A, Heptonstall J, et al. Ebolavirus and Marburgvirus: Insight the *Filoviridae* family. Mol Aspects Med **2008**; 29:151–85.
2. Klenk HD. Will we have and why do we need an Ebola vaccine? Nat Med **2000**; 6:1322–3.
3. Hartlieb B, Weissenhorn W. Filovirus assembly and budding. Virology **2006**; 344:64–70.
4. Mittler E, Kolesnikova L, Strecker T, Garten W, Becker S. Role of the transmembrane domain of Marburg virus surface protein GP in assembly of the viral envelope. J Virol **2007**; 81:3942–8.
5. Timmins J, Scianimanico S, Schoehn G, Weissenhorn W. Vesicular release of Ebola virus matrix protein VP40. Virology **2001**; 283:1–6.
6. Noda T, Sagara H, Suzuki E, Takada A, Kida H, Kawaoka Y. Ebola virus VP40 drives the formation of virus-like filamentous particles along with GP. J Virol **2002**; 76:4855–65.
7. Bavari S, Bosio CM, Wiegand E, et al. Lipid raft microdomains: A gateway for compartmentalized trafficking of Ebola and Marburg viruses. J Exp Med **2002**; 195:593–602.
8. Urata S, Noda T, Kawaoka Y, Morikawa S, Yokosawa H, Yasuda J. Interaction of Tsg101 with Marburg virus VP40 depends on the PPPY motif, but not the PT/SAP motif as in the case of Ebola virus, and Tsg101 plays a critical role in the budding of Marburg virus-like particles induced by VP40, NP, and GP. J Virol **2007**; 81:4895–9.
9. Dolnik O, Kolesnikova L, Becker S. Filoviruses: Interactions with the host cell. Cell Mol Life Sci **2008**; 65:756–76.
10. Dolnik O, Kolesnikova L, Stevermann L, Becker S. Tsg101 is recruited by a late domain of the nucleocapsid protein to support budding of Marburg virus-like particles. J Virol **2010**; 84:7847–56.
11. Liu Y, Harty RN. Viral and host proteins that modulate filovirus budding. Future Virol **2010**; 5:481–91.
12. Freed EO. Viral late domains. J Virol **2002**; 76:4679–87.
13. Craven RC, Harty RN, Paragas J, Palese P, Wills JW. Late domain function identified in the vesicular stomatitis virus M protein by use of rhabdovirus-retrovirus chimeras. J Virol **1999**; 73:3359–65.
14. Harty RN, Brown ME, Wang G, Huibregtse J, Hayes FP. A PPxY motif within the VP40 protein of Ebola virus interacts physically and functionally with a ubiquitin ligase: Implications for filovirus budding. Proc Natl Acad Sci U S A **2000**; 97:13871–6.
15. Jasenosky LD, Neumann G, Lukashevich I, Kawaoka Y. Ebola virus VP40-induced particle formation and association with the lipid bilayer. J Virol **2001**; 75:5205–14.
16. Licata JM, Simpson-Holley M, Wright NT, Han Z, Paragas J, Harty RN. Overlapping motifs (PTAP and PPEY) within the Ebola virus VP40 protein function independently as late budding domains: involvement of host proteins TSG101 and VPS-4. J Virol **2003**; 77:1812–9.
17. Timmins J, Schoehn G, Kohlhaas C, Klenk HD, Ruigrok RW, Weissenhorn W. Oligomerization and polymerization of the filovirus matrix protein VP40. Virology **2003**; 312:359–68.
18. Hoenen T, Biedenkopf N, Zielecki F, et al. Oligomerization of Ebola virus VP40 is essential for particle morphogenesis and regulation of viral transcription. J Virol **2010**; 84:7053–63.
19. Han Z, Boshra H, Sunyer JO, Zwiers SH, Paragas J, Harty RN. Biochemical and functional characterization of the Ebola virus VP24 protein: implications for a role in virus assembly and budding. J Virol **2003**; 77:1793–800.
20. Jasenosky LD, Kawaoka Y. Filovirus budding. Virus Res **2004**; 106:181–8.
21. Licata JM, Johnson RF, Han Z, Harty RN. Contribution of Ebola virus glycoprotein, nucleoprotein, and VP24 to budding of VP40 virus-like particles. J Virol **2004**; 78:7344–51.
22. Kaletsky RL, Francica JR, Agrawal-Gamse C, Bates P. Tetherin-mediated restriction of filovirus budding is antagonized by the Ebola glycoprotein. Proc Natl Acad Sci U S A **2009**; 106:2886–91.
23. Hu CD, Chinenov Y, Kerppola TK. Visualization of interactions among bZIP and Rel family proteins in living cells using bimolecular fluorescence complementation. Mol Cell **2002**; 9:789–98.
24. Kerppola TK. Visualization of molecular interactions by fluorescence complementation. Nat Rev Mol Cell Biol **2006**; 7:449–56.
25. Kerppola TK. Bimolecular fluorescence complementation: visualization of molecular interactions in living cells. Methods Cell Biol **2008**; 85:431–70.
26. Liu Y, Cocka L, Okumura A, Zhang YA, Sunyer JO, Harty RN. Conserved motifs within Ebola and Marburg virus VP40 proteins are important for stability, localization, and subsequent budding of virus-like particles. J Virol **2010**; 84:2294–303.
27. Watanabe S, Noda T, Kawaoka Y. Functional mapping of the nucleoprotein of Ebola virus. J Virol **2006**; 80:3743–51.
28. Noda T, Watanabe S, Sagara H, Kawaoka Y. Mapping of the VP40-binding regions of the nucleoprotein of Ebola virus. J Virol **2007**; 81:3554–62.